EXPERIMENTAL CELL RESEARCH 221, 311–319 (1995)

# Motility of Vinculin-Deficient F9 Embryonic Carcinoma Cells Analyzed by Video, Laser Confocal, and Reflection Interference Contrast Microscopy

WOLFGANG H. GOLDMANN,* MATHIAS SCHINDL,† TIMOTHY J. CARDOZO,* AND ROBERT M. EZZELL*,[1]

*Surgery Research Laboratory, Massachusetts General Hospital, Department of Surgery, Harvard Medical School, Charlestown, Massachusetts 02129; and †Biophysics E-22, Technical University of Munich, Germany

**We have studied the motility of wild-type F9 and vinculin-deficient (5.51) mouse embryonal carcinoma cells. F9 cells extended filopodia at a rate of 61 (±18) nm/s over a distance of 3.18 (±0.29) μm. In contrast, 5.51 cells exhibited filopodia which extended at a similar speed of 57 (±17) nm/s but over a longer distance of 5.10 (±2.14) μm. Cell–substratum contact areas of both cell types were examined by reflection interference contrast microscopy. Wild-type F9 cells had distinct close contacts (dark gray areas) at the cell periphery, whereas 5.51 cells had only a few light gray pinpoint contacts with the substrate. Confocal microscopy showed α-actinin to be localized along actin stress fibers in wild-type cells, and in 5.51 cells stress fibers were absent and α-actinin was associated with F-actin in the filopodia. $\beta_1$-integrin, talin, and paxillin were concentrated in focal contacts in wild-type cells, but in 5.51 cells $\beta_1$-integrin and talin were in patches under the plasma membrane and paxillin was diffusely distributed in the cytoplasm. We conclude that changes in cell shape and motility of 5.51 compared to wild-type F9 cells are due to the absence of vinculin even though there may be functions of other focal adhesion complex proteins, e.g., talin, linking the actin cytoskeleton to the plasma membrane.** © 1995 Academic Press, Inc.

## INTRODUCTION

The formation of actin-membrane attachments is a principal mechanism by which tissue cells determine their shape, attach to substrates, and direct their motility. One of the most thoroughly studied and possibly the most complicated connection between actin and the cell membrane is the complex of proteins and lipids that forms at sites where cells attach to the extracellular matrix. The transmembrane proteins of the integrin family are believed to be responsible for linking the actin cytoskeleton to the plasma membrane but the order, with which other proteins bind integrins, lipids, actin, or each other, is only partly understood and is still under investigation. The major protein components which assemble at sites of attachment of the cell to extracellular matrix are vinculin, talin, and α-actinin. These proteins are believed to form complexes with each other and with other components which serve to link filamentous actin to the membrane. Their molecular interactions are best understood in focal contacts (or adhesion plaques), specialized membrane regions for the attachment of cells to the extracellular matrix [1, 2].

Cell adhesion can be studied in model systems, e.g., using mouse F9 embryonal carcinoma cells. Samuels *et al.* [3] examined the motile behavior and distribution of vinculin and F-actin in mouse F9 embryonic carcinoma cell variants. They showed that F9 cells adhere to the substrate by first sending out long, thin projections, called filopodia. This is soon followed by veil-like lamellipodia which increase the area of the cell's attachment to the substrate. In comparison, 5.51 cells—a vinculin-deficient F9 variant—show numerous actively extending and retracting filopodia, but no lamellipodia. In wild-type F9 cells, F-actin is organized into bundles (stress fibers) which terminate at focal contacts containing vinculin. In contrast, 5.51 cells exhibit no actin stress fibers and no detectable vinculin protein; instead F-actin was concentrated under the plasma membrane and in filopodia. These findings suggest that vinculin is required for cell attachment and spreading as well as for the formation of stress fibers. In this work we have used time-lapse video, laser confocal, and reflection interference contrast microscopy combined with digital image analysis to study the dynamics of filopod motility and the formation of focal adhesion complexes in wild-type and vinculin-deficient F9 cell lines.

## MATERIALS AND METHODS

*Cell culture.* Wild-type F9 embryonal carcinoma cells were maintained on 1% gelatin-coated charged plastic culture dishes in high-

[1] To whom correspondence and reprint requests should be addressed.



0014-4827/95 $12.00

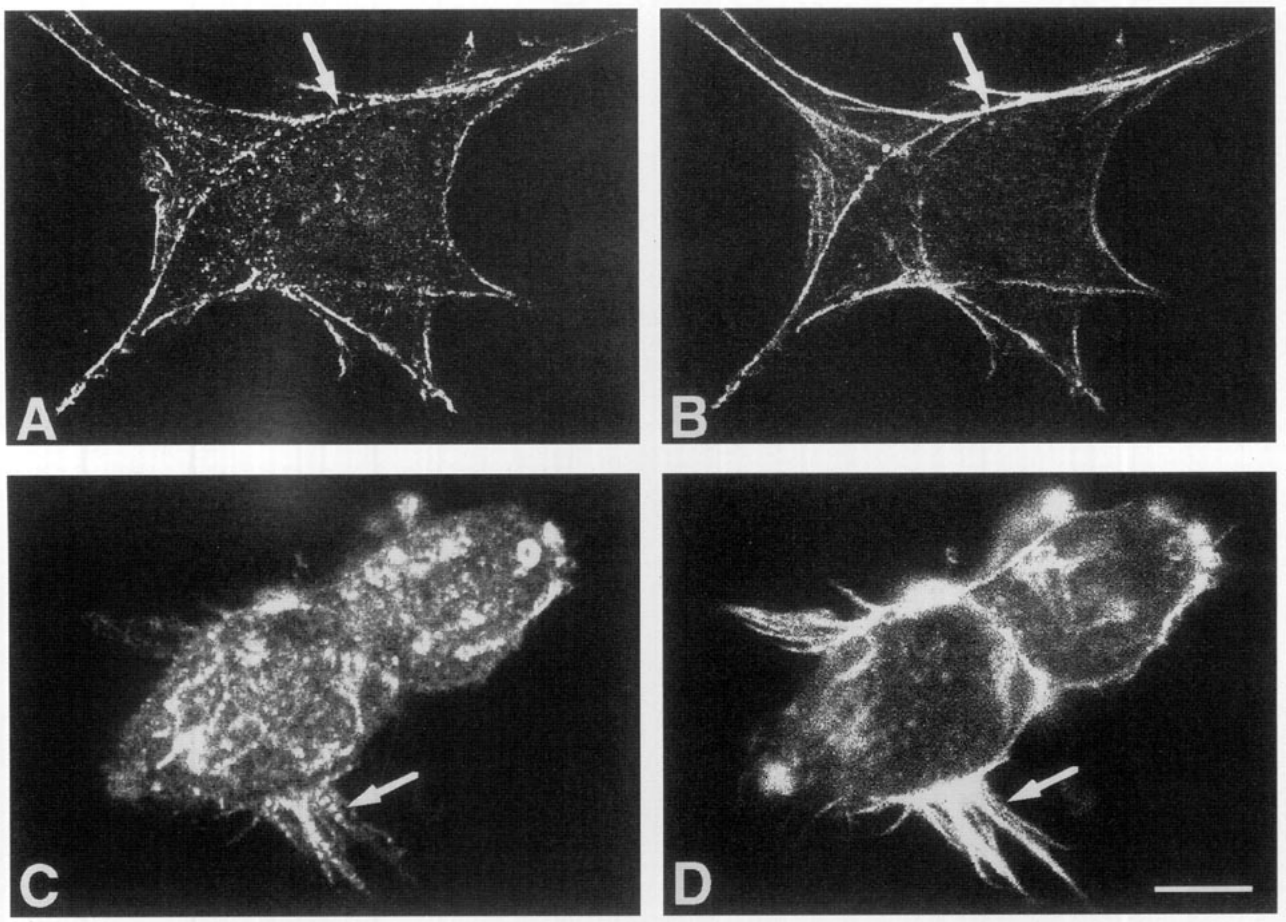


**FIG. 1.** Colocalization of $\alpha$-actinin (A, C) and F-actin (B, D) in wild-type F9 (A, B) and 5.51 (C, D) cells. Cells were stained with a mouse monoclonal antibody to $\alpha$-actinin and then with rhodamine–phalloidin. In wild-type cells, $\alpha$-actinin was associated with stress fibers in a stippled pattern (arrows in A, B). In 5.51 cells, $\alpha$-actinin had a similar stippled pattern associated with F-actin in the cytoplasm and filopodia (arrows in C, D). C and D show two 5.51 cells in contact. Bar (in D), 4 $\mu$m for A, B; and 3 $\mu$m for C, D.

glucose (4.5 g/liter) Dulbecco's modified Eagle's medium supplemented with 10% calf serum and 1% L-glutamine, 1 mg/ml penicillin and streptomycin. The vinculin-deficient cell line (5.51) was produced by ethanemethylsulfonate (EMS) mutagenesis of the F9 cells [3]. The 5.51 cells, which express only 5′ portions of vinculin mRNA which is not translated, appear to have a normal pair of vinculin genes based on Southern blotting [4]. The 5.51 cell line was cultured in suspension in the same medium as the wild-type cells [5]. For immunofluorescence and imaging studies, both cell lines were plated on 24-mm$^2$ No. 1 glass coverslips coated with 10 $\mu$g/ml bovine fibronectin and 2 $\mu$g/ml polylysine and examined 3 to 4 h later. Since 5.51 cells do not adhere to substrates, polylysine was used to immobilize them for study. Fibronectin was added to promote integrin-based adhesion of the wild-type F9 cells.

*Time-lapse video microscopy.* Time-lapse video microscopy was performed as previously described by Samuels *et al.* [3]. In short, wild-type F9 and mutant 5.51 cells were cultured on 25-mm circular coverslips coated with 10 $\mu$g/ml fibronectin and 2 $\mu$g/ml polylysine. The cells were maintained in a Leiden coverslip chamber and examined in a Zeiss Axiovert inverted microscope, using a 100X Plan-Neofluar objective and Nomarski differential interference contrast (DIC) optics. A Zeiss environmental microscope chamber was used to maintain the cell culture at 37°C and 5% $CO_2$. Video images obtained with a Hamamatsu C2400 Newvicon camera were recorded onto a Sony LVR 5000 laserdisk recorder at 2-s intervals.

*Immunofluorescence and laser confocal microscopy.* F9 cell lines were cultured on glass coverslips coated with fibronectin and polylysine as described above. Twelve hours after plating, the cells were fixed in 4% paraformaldehyde for 15 min followed by three washes in phosphate-buffered saline (PBS, pH 7.4) and extracted for 2 min in 0.2% Triton X-100. All procedures were done at room temperature (~22°C). Following extraction, cells were washed for 10 min in PBS and then placed in a blocking solution containing 3% BSA and 1% normal donkey serum (to reduce nonspecific antibody binding) for 1 h. Cells were then incubated for 1 h in antibodies to $\alpha$-actinin, talin, paxillin, or $\beta_1$-integrin, washed three times (15 min each) in PBS and incubated for 1 h in 10 mg/ml fluorescein-conjugated donkey anti-rabbit IgG (for staining talin and $\beta_1$-integrin) or donkey anti-F(ab)$_2$ fragment of mouse IgG or IgM (for staining paxillin and $\alpha$-actinin, respectively). The coverslips were washed 12 h in PBS, and then stained with rhodamine phalloidin (diluted 1:100 in PBS). After staining, the coverslips were washed in PBS (three changes, 15 min each) and a drop of 1% *n*-propyl-gallate (used to reduce photobleaching of fluorescence, Sigma Chemical Co., St. Louis, MO) in an 8:2

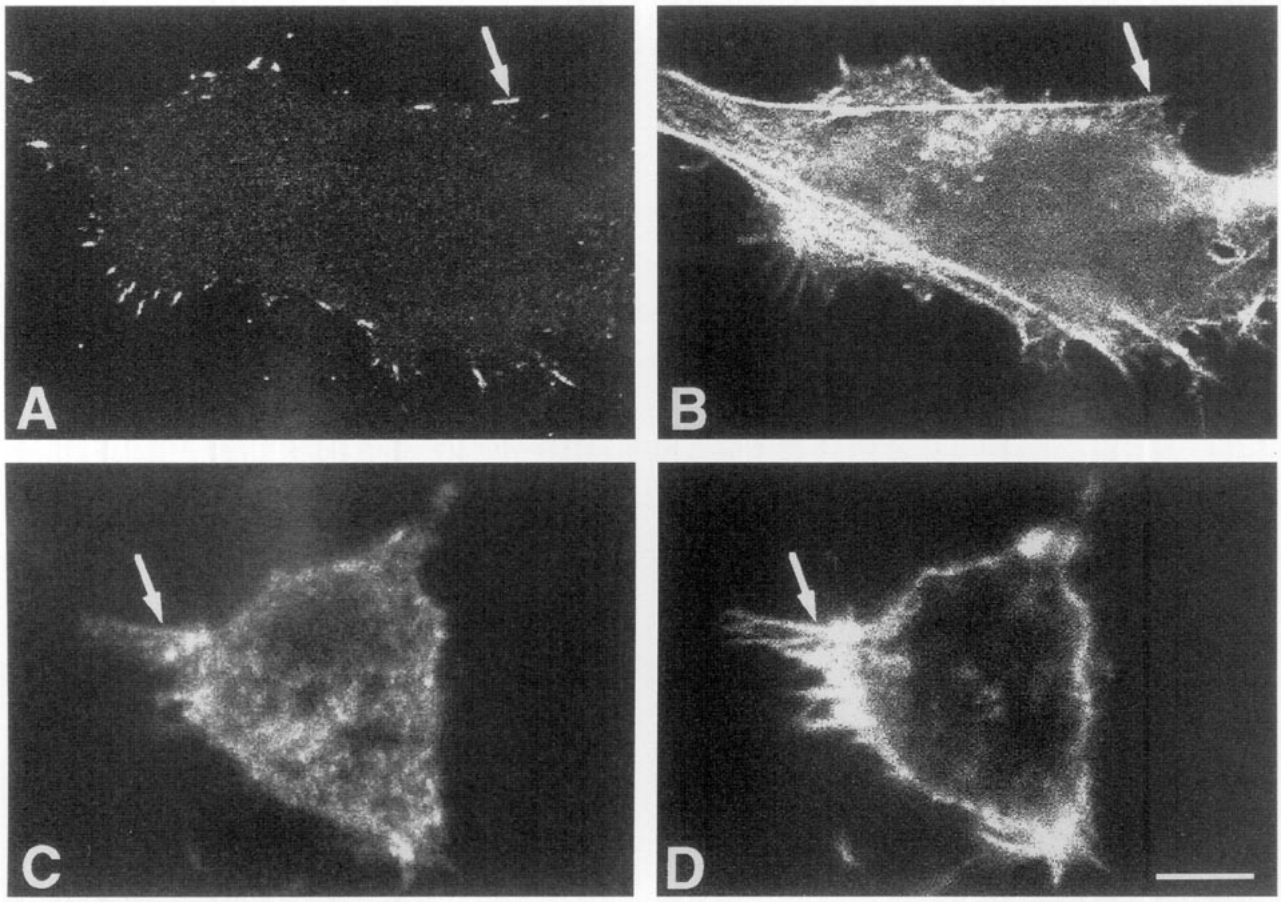


**FIG. 2.** Colocalization of paxillin (A, C) and F-actin (B, D) in wild-type F9 (A, B) and 5.51 (C, D) cells. Cells were stained with a mouse monoclonal antibody to paxillin and then with rhodamine–phalloidin. In wild-type cells, paxillin was concentrated at the ends of stress fibers in focal contacts (arrows in A, B). In 5.51 cells, paxillin was diffusely distributed in the cytoplasm, including filopodia (arrows in C, D). Bar (in D), 4 $\mu$m for A, B; and 3 $\mu$m for C, D.

mixture of glycerol and PBS (pH 8.5) was added to each coverslip before sealing it with nail polish. The samples were examined using a confocal imaging system (Bio-Rad MRC 600 attached to a Zeiss Axiovert inverted microscope (Carl Zeiss Inc., Thornwood, NY) with a 100X Zeiss Plan-Neofluar objective.

For three-dimensional reconstructions of the confocal images, 70 optical sections at 0.25-$\mu$m intervals of the entire thickness of the cell (including the area above and below it) were collected using a Zeiss IM35 inverted microscope, 100X Planeofluor objective, Bio-Rad MRC 600 confocal microscope and COMOS software. The stack of confocal images was then compiled and rendered at three-degree increments to provide a 360° view of the cell using Image-1 software running on a 486, 50 MHz PC (Universal Imaging Corp., West Chester, PA).

*Reflection interference contrast microscopy.* Reflection interference contrast microscopy (RICM) was carried out as described by Rädler and Sackmann [6] and Schindl *et al.* [7]. The system consisted of an Zeiss Axiomat inverted microscope containing a 63X antiflex Neofluar objective, a mercury arc lamp, and custom optics for observing RICM and bright-field images alternatively or in parallel. Filters were used to reduce exposure to ultraviolet and infra-red light and to select the 546-nm green mercury line. The interference images were captured using a CCD camera (HR-480, Aqua-TV, D-87437 Kempten, Germany) and recorded onto a Panasonic AG-7350 video tape recorder.

*Video image processing.* Digital image processing was done using an Apple Macintosh Quadra 950 equipped with an accelerated video display card (Futura LX, Radius, Sunnyvale, CA) and PixelTools video digitizing cards (Perceptics, Knoxville, TN). Image analysis was done using Image VDM Software (Perceptics) based on the public domain image processing software "NIH Image" (written by Wayne Rasban, NIH, Bethesda, MD). Measurements of filopod movement were carried out using a custom extension installed in NIH Image called "Object Image" software, as described by Vischer *et al.* [8].

## RESULTS

### *Immunolocalization of Focal Adhesion Complex Proteins*

The F9 cell lines were stained with antibodies to $\alpha$-actinin, paxillin, talin, and $\beta_1$-integrin and the localiza-

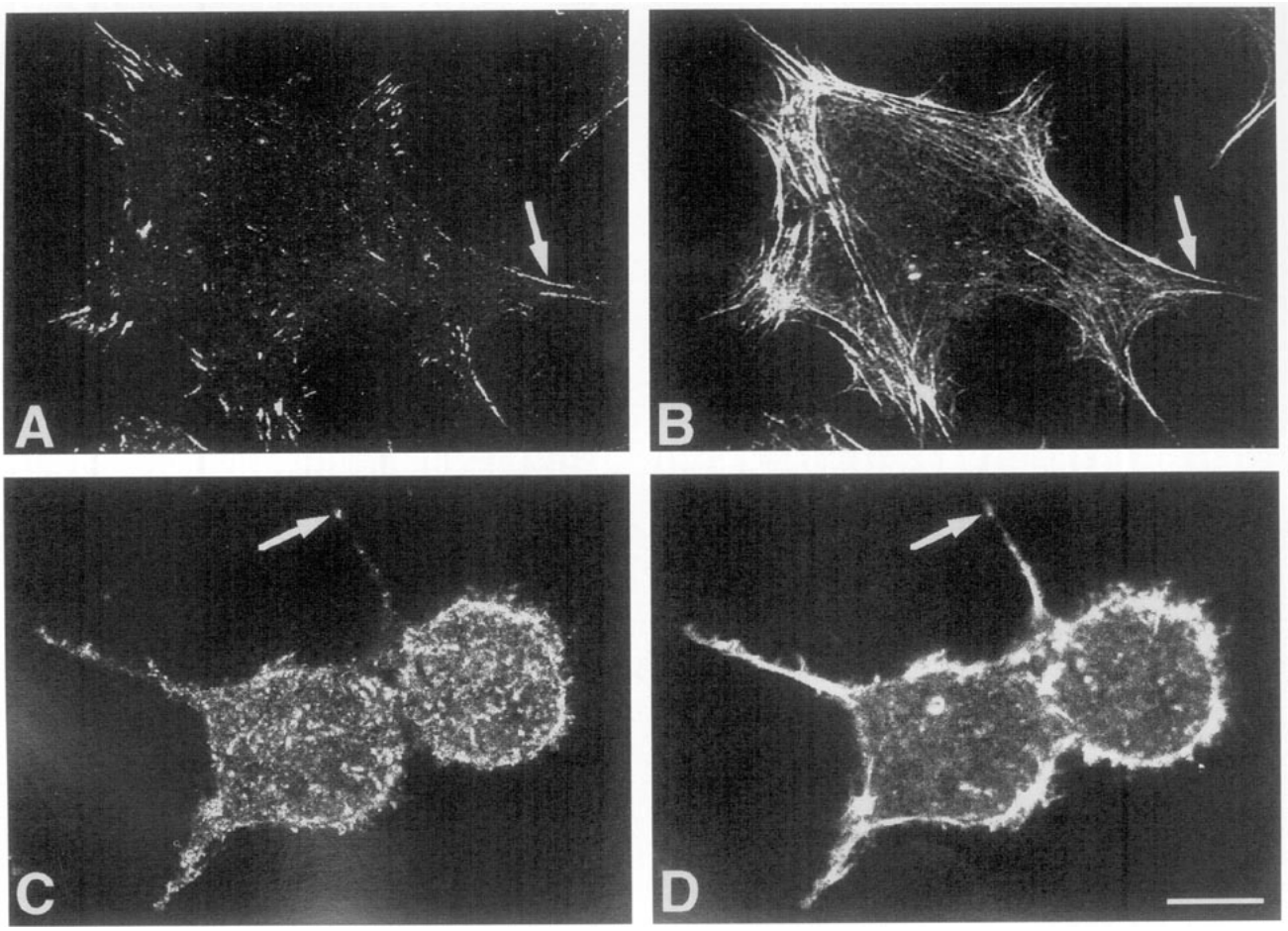


**FIG. 3.** Colocalization of talin (A, C) and F-actin (B, D) in wild-type F9 (A, B) and 5.51 (C, D) cells. Cells were stained with a rabbit polyclonal antibody to talin and then with rhodamine–phalloidin. In wild-type cells, talin was concentrated at the ends of stress fibers in focal contacts (arrows in A, B). In 5.51 cells, talin was present in patches throughout the cell, including filopodia (arrows in C, D). C and D show two 5.51 cells in contact. Bar (in D), 4 $\mu$m for A, B; and 3 $\mu$m for C, D.

tion of these proteins was compared with the distribution of F-actin. In wild-type F9 cells, $\alpha$-actinin was distributed at intervals along actin stress fibers and was concentrated in focal contacts (Fig. 1). In the vinculin-deficient 5.51 cells, $\alpha$-actinin colocalized with F-actin in the cell cortex and in filopodia. The same stippled staining pattern seen in wild-type F9 cells was observed in the 5.51 cells. Since the distribution of $\alpha$-actinin in all the F9 cell lines was determined by the organization of F-actin, the interaction of $\alpha$-actinin with F-actin did not appear to be effected by the loss of vinculin.

In the wild-type F9 cells, paxillin, talin, and $\beta_1$-integrin were all concentrated in focal contacts at the ends of stress fibers (Figs. 2–4). In 5.51 cells, however, talin and $\beta_1$-integrin colocalized with F-actin in patches near the plasma membrane, and paxillin was diffusely distributed in the cytoplasm. Since paxillin is known to bind to vinculin [9, 10], the diffuse distribution of paxillin in 5.51 cells may be directly due to the absence of vinculin.

### *Reflection Interference Contrast Microscopy (RICM)*

Wild-type F9 cells formed distinct filopodia and clearly visible lamellipodia after plating on the substrate. This was observed by RICM and bright-field optics (Fig. 5). RICM examination showed large dark gray areas, corresponding to close cell-substrate contacts. Dark streaks appearing at the cell periphery could be identified as focal contacts by varying the illumination aperture. Increasing the amount of polylysine in the substrate (up to 20 $\mu$g/ml) resulted in larger areas of close contacts in the wild-type cells.

Vinculin-deficient 5.51 cells were more rounded and spread less in comparison to wild-type cells. This was

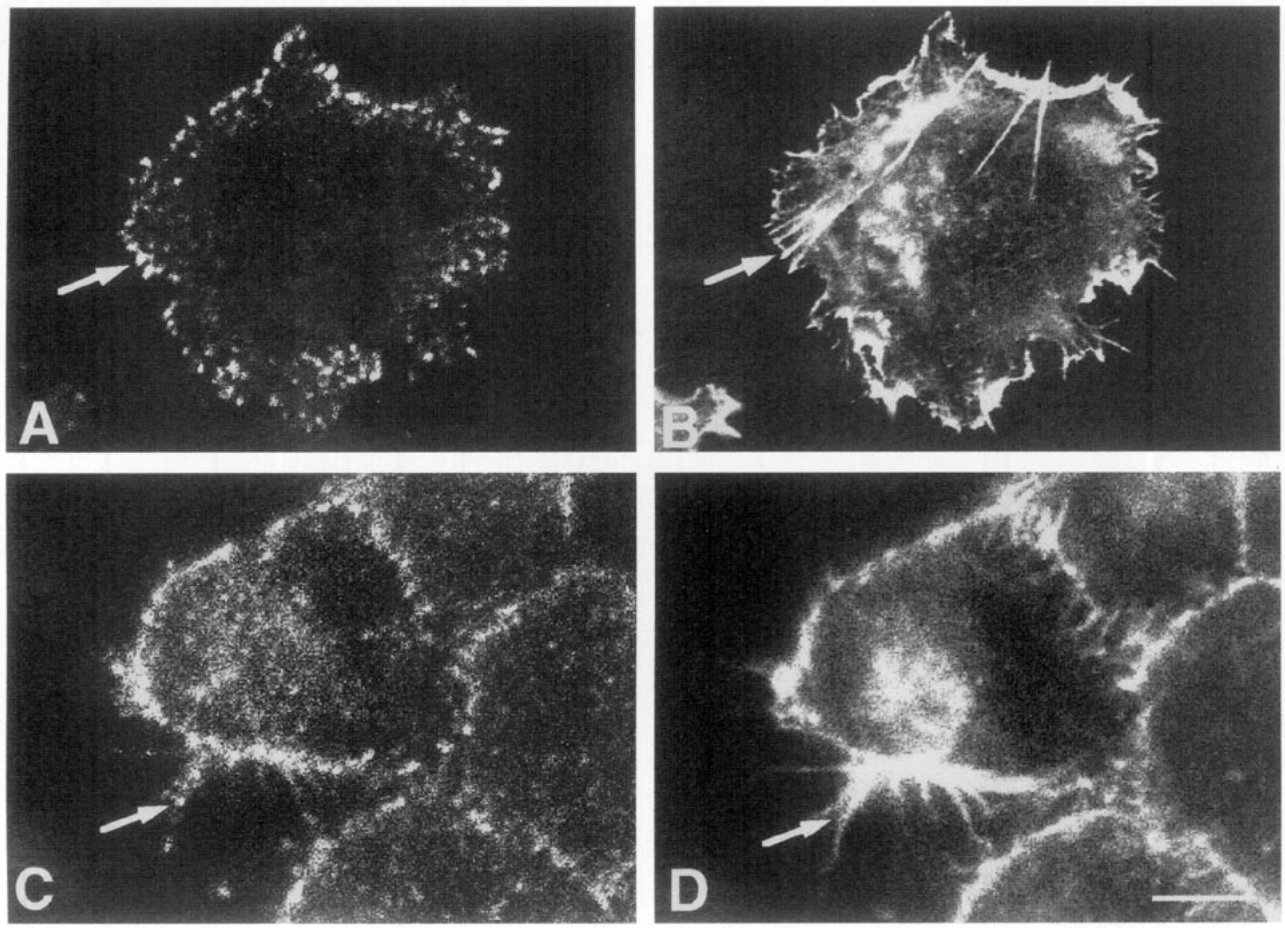


**FIG. 4.** Colocalization of $\beta_1$-integrin (A, C) and F-actin (B, D) in wild-type F9 (A, B) and 5.51 (C, D) cells. Cells were stained with a rabbit polyclonal antibody to $\beta_1$-integrin and then with rhodamine–phalloidin. $\beta_1$-integrin was concentrated at the ends of stress fibers in focal contacts in wild-type cells (arrows in A, B). In 5.51 cells, $\beta_1$-integrin was present in patches near the plasma membrane and in filopodia (arrows in C, D). C and D show a cluster of four 5.51 cells. Bar (in D), 4 $\mu$m for A, B; and 2 $\mu$m for C, D.

due to the absence of lamellipodia and fewer filopodia in 5.51 cells compared to the wild-type cells. RICM examination showed the 5.51 cells to have small pinpoint dark gray spots localized underneath the central part of the cell, indicating poorly formed focal contacts (see Fig. 5). The areas of contact differed substantially from the outer perimeter of the cell in both RICM and bright-field views. These small areas of contact increased only slightly with increasing polylysine concentration.

### *Filopodia Motility Analyzed by Time-Lapse Video Microscopy*

The motion of cells is based on the combined forces of various cell extensions. We used time-lapse video microscopy to compare the formation of filopodia in wild-type F9 and mutant 5.51 cells plated on fibronectin and polylysine-coated coverslips (Fig. 6). In both cell types, filopodia extended out from the cell body at a constant and similar speed (Fig. 7). In 5.51 cells filopodia protruded for a longer duration than in wild-type cells which resulted in longer filopodia. This is summarized in Table 1.

### *F-Actin Organization*

Laser confocal microscopy was used to examine the three-dimensional organization of actin in F9 cells stained with rhodamine–phalloidin (Fig. 8). Viewing the wild-type F9 cell at several angles showed F-actin to be organized into filament bundles (i.e., stress fibers) that spanned the ventral surface of the cell and terminated in focal contacts. In contrast, the 5.51 cells lacked stress fibers and actin was concentrated in filopodia and in patches near the plasma membrane. The ab-

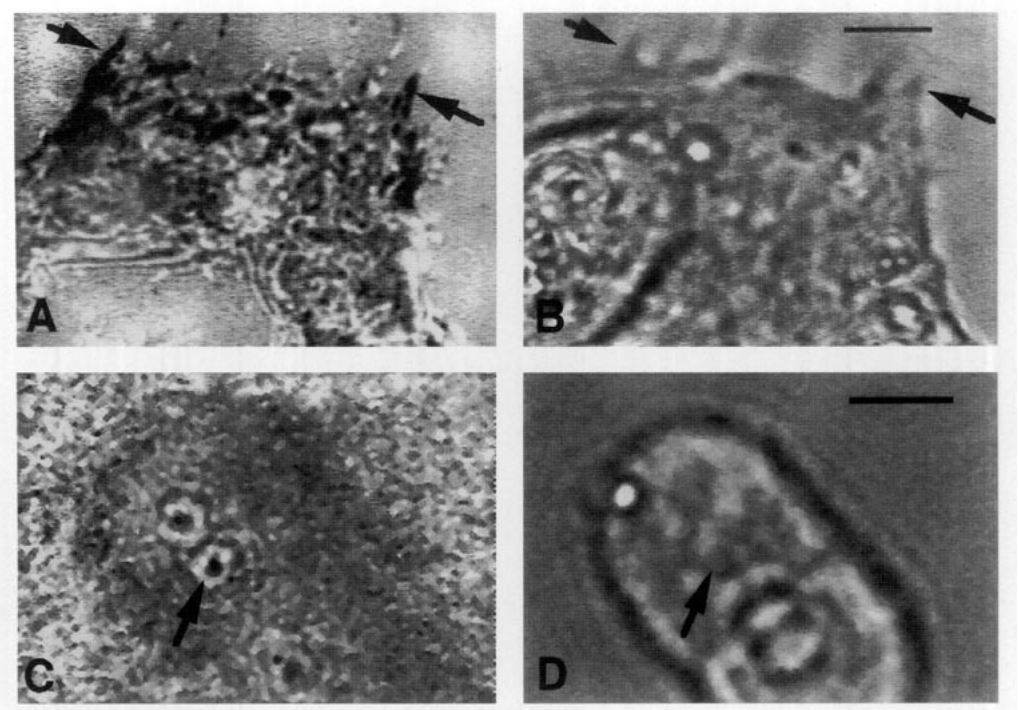


**FIG. 5.** Reflection interference contrast microscopy (RICM; A, C) and corresponding bright-field images (B, D) of wild-type F9 (A, B) and 5.51 (C, D) cells. RICM of wild-type cells show dark gray areas corresponding to close contacts and dark streaks at the cell periphery corresponding to focal contacts (arrows in A, B). 5.51 cells have a rounded morphology and RICM shows only small circular close contacts (arrows in C, D). Bars (in B, D), 5 $\mu$m.

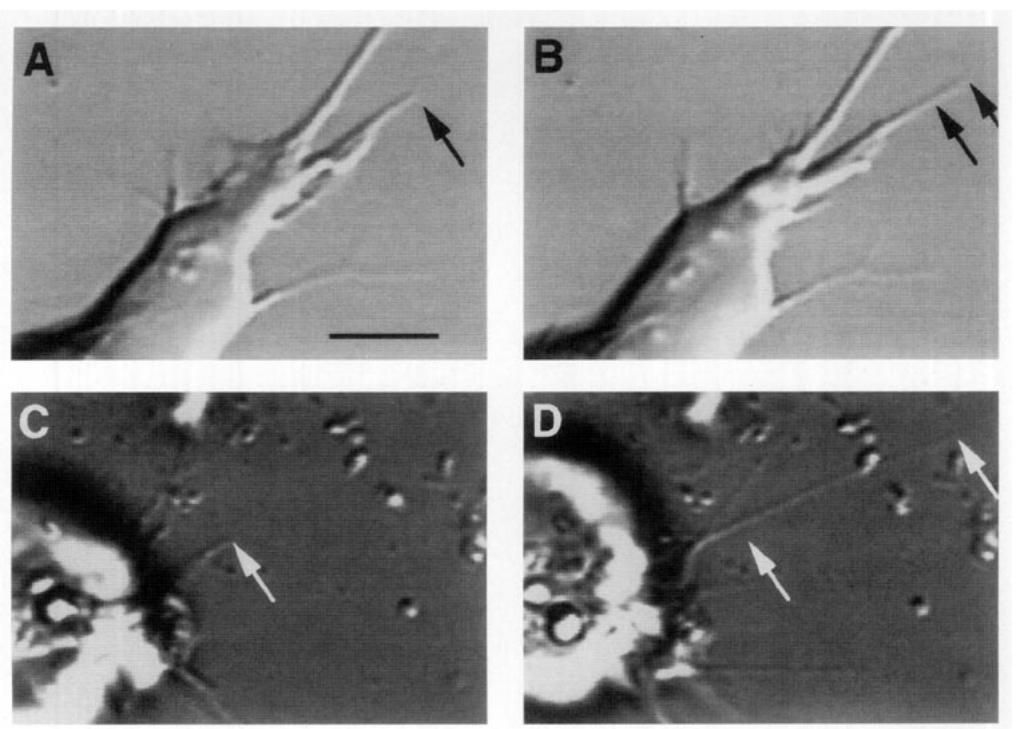


**FIG. 6.** Morphology of wild-type F9 (A, B) and 5.51 (C, D) cells examined using Nomarski differential interference contrast optics. The arrows show the beginning and ending positions of extending filopodia at 15-s intervals. Bar (in A), 5 $\mu$m.

sence of stress fibers in 5.51 cells was consistent with their spherical shape and lack of lamellipodia.

## DISCUSSION

This study shows that focal adhesion complex formation, actin organization, and cell motility are effected by the amount of vinculin in F9 cells. The vinculin-deficient 5.51 cell phenotype can be considered as (i) a distinct phenotype induced by the loss of vinculin, or (ii) the wild-type phenotype restricted to certain behaviors by the loss of vinculin. The results suggest that the latter possibility is indicated; i.e., 5.51 cells are wild-type cells arrested in the early stages of adhesion and spreading due to the absence of vinculin.

In wild-type cells the cytoskeleton is linked to the plasma membrane. This interaction may play a central role in regulating cell shape and size. In order to obtain information on the role of vinculin in these processes, we have utilized a vinculin-deficient cell line which is missing an important linkage of actin filaments to the plasma membrane. The formation of filopodia in wild-type F9 cells is characterized by linear growth. This behavior has also been observed in *Dictyostelium* cells [7] and has been discussed generally for mammalian cells by Stossel [11]. In 5.51 cells, filopodia formation was similar to wild-type cells, but filopodia were significantly fewer and longer. This finding confirms previous observations by laser confocal microscopy of F9 cells stained for vinculin and F-actin that newly formed filopodia can probably be stabilized by the involvement of vinculin anchoring actin filaments to the plasma membrane [3]. This supports a model in which during filopod formation vinculin provides structure and stability by linking actin filaments to the plasma membrane [1].

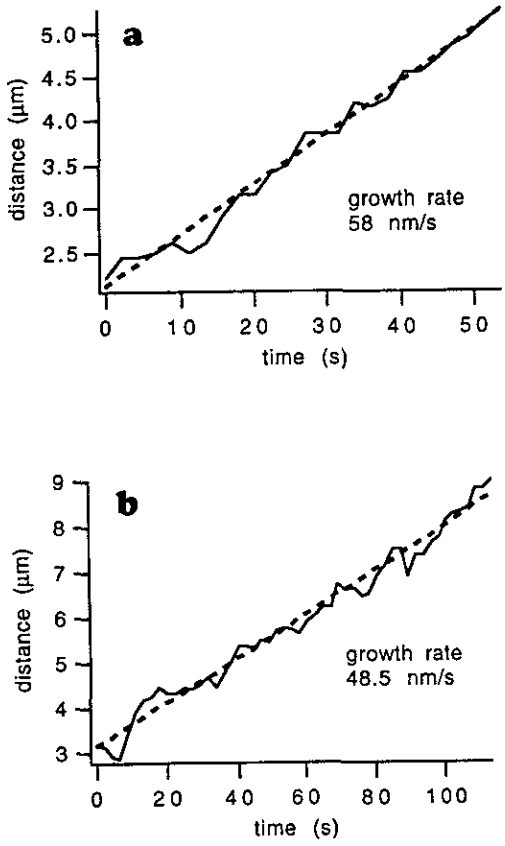


**FIG. 7.** Graph showing a plot of distance versus time of extending filopodia in wild-type F9 (a) and 5.51 cells (b). See Fig. 6 for example of filopodia used for measurements. The rate of filopodia growth was 58 nm/s for wild-type F9 cells, and 48.5 nm/s for 5.51 cells.

**TABLE 1**

Distance, Duration of Extension and Speed of Filopod Growth of Wild-Type F9 and 5.51 Cells. The Standard Deviation and Number of Measurements per Cells Are Shown in Parentheses

| Cell type | Distance [μm] | Duration [s] | Speed [nm/s] | No. of cells |
|---|---|---|---|---|
| F9 | 3.18 (±0.29; 14) | 56.4 (±20.4; 14) | 61 (±18; 14) | 7 |
| 5.51 | 5.10 (±2.14; 12) | 85.0 (±40.0; 12) | 57 (±17; 12) | 6 |

The differences in the formation of cell-substrate contacts in wild-type F9 and 5.51 cells can be considered theoretically: cell shape changes are normally controlled by bending stiffness and shear elasticity of the plasma membrane which is effected by the binding of the actin cytoskeleton to proteins in the lipid bilayer. If the shear elasticity is ignored the feature of adhesion in these cells can be explained in terms of the general minimum bending energy concept of shape changes that occur during cell adhesion [12]. This concept predicts energy contributions for cell curvature, adhesion, extension, and energy associated with volume and pressure changes. Our results suggest that the longer filopodia in 5.51 cells compared to wild-type cells is probably due to a decrease in bending stiffness of the plasma membrane which is caused by the lack of vinculin. Varnum-Finney and Reichardt [13] have also observed differences in the formation of cell expansions, using the neuronal cell line PC12 transfected with a vector expressing antisense vinculin RNA to reduce vinculin protein. They found that in vinculin-deficient PC12 cells growth cones advanced more slowly and filopodia and lamellipodia were less stable in comparison to control cells. Volberg *et al.* [14], using the vinculin-deficient F9 cell line γ229, showed that substrate adhesion is impaired and cell spreading is reduced, but that the formation of focal adhesions is not effected. The absence of defined focal adhesions we observe may be

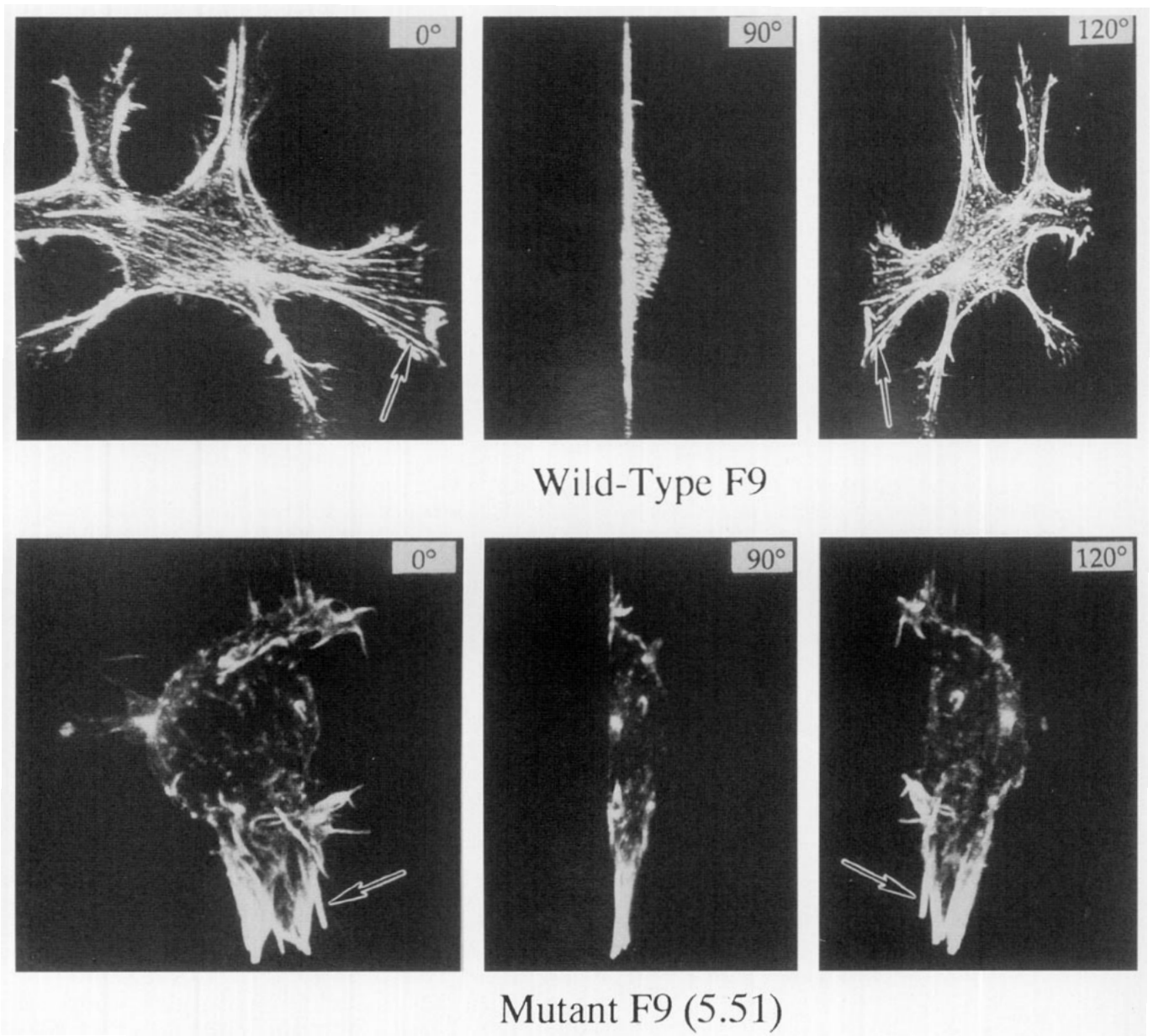


**FIG. 8.** Three-dimensional reconstruction of confocal images of a wild-type F9 (upper panels) and 5.51 cell (lower panels) stained with rhodamine–phalloidin to localize actin filaments. Different orientations were produced by compiling digitized confocal sections (acquired at 0.16-$\mu$m intervals) to create images at 0° (from the top), 90° (from the side), and 120° (under the substrate) views. In the wild-type F9 cell, actin-containing stress fibers (arrow) were located close to the substrate and terminate at the cell periphery in focal contacts. The 5.51 cell lacks stress fibers and does not spread. Actin in these cells is concentrated in long filopodia (arrow). Arrows in 0° and 120° views point to same structures.

due to different methods used to inactivate the vinculin gene in $\gamma$229 and 5.51 cells. We agree with these authors [14] that the interaction of actin with the plasma membrane in focal contacts may involve proteins other than vinculin, e.g., talin, $\alpha$-actinin, and $\beta_1$-integrin. These proteins are all expressed in the 5.51 cells. In order to fully understand the assembly of the focal adhesion complex more comprehensive work has to be carried out to elucidate the individual function of the proteins and the interactions between them.

We thank Dr. Eileen Adamson (La Jolla Cancer Research Foundation) for her encouragement and helpful insights, Dr. Keith Burridge (University of North Carolina) for providing the talin antibodies, and

Ms. K. Scharpf (Technical University of Munich) for helping with the experiments. This work was supported by grants to R.M.E. from the Muscular Dystrophy Association, Crohn's and Colitis Foundation of America, American Cancer Society, Deutsche Forschungsgemeinschaft (W.H.G. and M.S.), and NATO CRG 940 666 (W.H.G. and R.M.E.).

## REFERENCES

1. Condeelis, J. (1993) *Annu. Rev. Cell Biol.* **9,** 411–444.
2. Isenberg, G., and Goldmann, W. H. (1995) *in* The Cytoskeleton, Structure and Assembly (Hesketh, J., and Pryme, I., Eds.), Vol. 1, pp. 169–204, JAI Press, Greenwich, CT, USA.
3. Samuels, M., Ezzell, R. M., Cardozo, T. J., Critchley, D. R., Coll, J. L., and Adamson, E. D. (1993) *J. Cell Biol.* **121,** 909–921.
4. Grover, A., Rosenstraus, M. J., Sterman, B., Snook, M. E., and Adamson, E. D. (1987) *Dev. Biol.* **119,** 1–11.
5. Adamson, E. D., Baribault, H., and Kemler, R. (1990) *Dev. Biol.* **138,** 338–347.
6. Rädler, J., and Sackmann, E. (1993) *J. Phys. Orsay Fr.* **3,** 727–748.
7. Schindl, M., Wallraff, E., Deubzer, B., Witke, W., Gerisch, G., and Sackmann, E. (1995) *Biophys. J.* **68,** 1177–1190.
8. Vischer, N. O. E., Huls, P. G., and Woldringh, C. L. (1994) *Binary* **6,** 160–166.
9. Turner, C. E., Glenney, J. R., Jr., and Burridge, K. (1990) *J. Cell Biol.* **111,** 1059–1068.
10. Wood, C. K., Turner, C. E., Jackson, P., and Critchley, D. R. (1994) *J. Cell Sci.* **107,** 709–717.
11. Stossel, T. P. (1993) *Science* **260,** 1086–1094.
12. Seifert, U., and Lipowsky, R. (1990) *Phys. Rev. A* **42,** 4768–4771.
13. Varnum-Finney, B., and Reichardt, L. F. (1994) *J. Cell Biol.* **127,** 1071–1084.
14. Volberg, T., Geiger, B., Kam, Z., Pankov, R., Simcha, I., Sabanay, H., Coll, J. L., Adamson, E., and Ben-Ze'ev, A. (1995) *J. Cell Sci.* **108,** 2253–2260.

Received June 19, 1995
Revised version received August 23, 1995